Surfactant-assisted epitaxial growth and magnetism of Fe films on Cu(111)



2008 J. Phys.: Condens. Matter 20 265008

(http://iopscience.iop.org/0953-8984/20/26/265008)

J. Phys.: Condens. Matter **20** (2008) 265008 (8pp) doi:10.1088/0953-8984/20/26/265008

# Surfactant-assisted epitaxial growth and magnetism of Fe films on Cu(111)

**M Á Niño[1,5], J Camarero[1], L Gómez[2], J Ferrón[3], J J de Miguel[1] and R Miranda[1,4]**

[1] Departamento de Física de la Materia Condensada and Instituto de Ciencia de Materiales 'Nicolás Cabrera', Universidad Autónoma de Madrid, Cantoblanco, 28049-Madrid, Spain
[2] Facultad de Ciencias Exactas, Ingeniería y Agrimensura, Instituto de Física Rosario, 2000-Rosario, Argentina
[3] Instituto de Desarrollo Tecnológico para la Industria Química (CONICET-UNL), Departamento de Materiales, Facultad de Ingeniería Química, UNL, 3000 Santa Fe, Argentina
[4] Instituto Madrileño de Estudios Avanzados en Nanociencia (IMDEA Nanociencia), Cantoblanco, 28049-Madrid, Spain

Received 11 March 2008, in final form 2 May 2008
Published 28 May 2008
Online at stacks.iop.org/JPhysCM/20/265008

**Abstract**
The magnetic properties of thin epitaxial layers of Fe grown on Cu(111) depend sensitively on the films' structure and morphology. A combination of experiments and numerical simulations reveals that the use of a surfactant monolayer (ML) of Pb during molecular beam epitaxy (MBE) growth at room temperature reduces the amount of interdiffusion at the Cu–Fe interface, retards the fcc-to-bcc transformation by about 2 ML and substantially increases the films' coercivity. The origin of all these alterations to the magnetic behavior can be traced back to the structural modifications provoked by the surfactant during the early growth stages. These results open the way for the controlled fabrication of custom-designed materials with specific magnetic characteristics.

(Some figures in this article are in colour only in the electronic version)

## 1. Introduction

The growth of ultrathin epitaxial layers of Fe on the compact faces of Cu, most notably Cu(100) and Cu(111), has attracted strong interest recently, with the main goal of attempting to stabilize the fcc ($\gamma$) phase of Fe [1–4] and explore its predicted rich magnetic phase diagram [5, 6].

On Cu(111) Fe starts growing with fcc structure and pseudomorphically with the substrate [7–9] and then transforms to bcc with a compact (110) face as its thickness increases. Scanning tunneling microscopy (STM) experiments have demonstrated that the growth proceeds by forming three-dimensional islands from the beginning [10, 11]; these islands have at least double atomic height at the interface, a behavior analogous to what has already been described for epitaxial Co films on the same substrate [12]. The double-layer islands result from a process of intermixing between the deposit (Fe in this case) and the Cu substrate [13], whereas the rough growth front is due to the existence of Ehrlich–Schwoebel barriers at the step edges hindering interlayer diffusion [14, 15]. The combination of all these factors results in very rough films with a high density of structural defects, and a complicated succession of magnetic phases.

Our purpose in this work is to study in detail the influence of a surfactant (Pb) layer on the growth of the epitaxial Fe films on Cu(111) and the influence of those structural and morphological modifications on the films' magnetic properties, as a first step towards a controlled tailoring of the system's magnetic behavior.

## 2. Experimental details

The experiments have been carried out in an ultra high vacuum (UHV) system with two sections: the first one is dedicated to the growth and structural characterization of the epitaxial films, and is equipped with molecular beam epitaxy (MBE) evaporators and facilities for low energy electron diffraction (LEED), Auger electron spectroscopy (AES) and neutral He atom diffraction, plus sample manipulation and cleaning.

[5] Present address: Sincrotrone Trieste S.C.p.A., S.S. 14, km 163.5 in Area Science Park, 34012 Basovizza, Trieste, Italy.

 

The substrate used in all the experiments reported in this paper was a Cu(111) single crystal. It has a miscut angle of ∼1° and has been used in UHV for several years. It was routinely cleaned by cycles of $Ar^+$ bombardment (500 eV, 5 $\mu$A cm$^{-2}$) and annealing at 500 °C. Heating was accomplished by means of a ceramic heater in direct contact with the back of the crystal. The sample temperature was determined by a chromel–alumel thermocouple pressed against the crystal edge.

Cu and Pb were evaporated from water-cooled Knudsen cells. The crucible temperatures were measured by thermocouples attached to them; these readings were fed to temperature controllers which regulated the output of the power supplies. For Fe we used home-made electron bombardment evaporators, also equipped with water-cooled shrouds. The deposition rates have been calibrated from the layer-by-layer intensity oscillations observed in the experiments employing Pb as surfactant [16].

The morphology of the growing films has been characterized by thermal energy atom scattering (TEAS), by monitoring the intensity of the specular beam in real time during deposition. This peak contains all the relevant information about the height distribution on the surface, which can be deduced from the experimental data by means of a well-established procedure that we have demonstrated in previous work [17].

The films' magnetic behavior was determined by magneto-optic Kerr Effect (MOKE) measurements, performed *in situ* within the second UHV chamber, which is directly connected to the first one; the samples can be transferred between both vessels without breaking the vacuum. Our experimental setup allows for MOKE measurements under both polar and longitudinal geometries, with a maximum applied field of 600 Oe.

## 3. Structural and morphological characterization during growth

### *3.1. Growth of Fe films on Cu(111) without surfactant*

Our experimental method for the characterization of growth is exemplified by the TEAS measurements presented in figure 1(a). The surface reflectivity for the impinging beam of neutral He atoms (dots) is monitored in real time during deposition of Fe at room temperature (RT); these data are then fitted in an iterative procedure, using a kinetic growth model determined by several adjustable parameters [17]. The result of this fit is shown with the continuous red line superimposed on the data points. As the outcome of this calculation, we obtain the evolution of the atomic layer fillings, which are plotted in figure 1(b) as a function of the total deposited thickness. The Fe film morphology described by these curves agrees well with previous reports [2–4] and presents two outstanding characteristics: the initial formation of islands with double atomic height at the Fe–Cu interface (represented by the curve labeled '1 + 2' in figure 1(b)), followed by the early occupation of the third and higher atomic levels and a growth of Fe with negligible interlayer diffusion, which results in atomic layer fillings following a Poisson distribution [18]. Such a growth

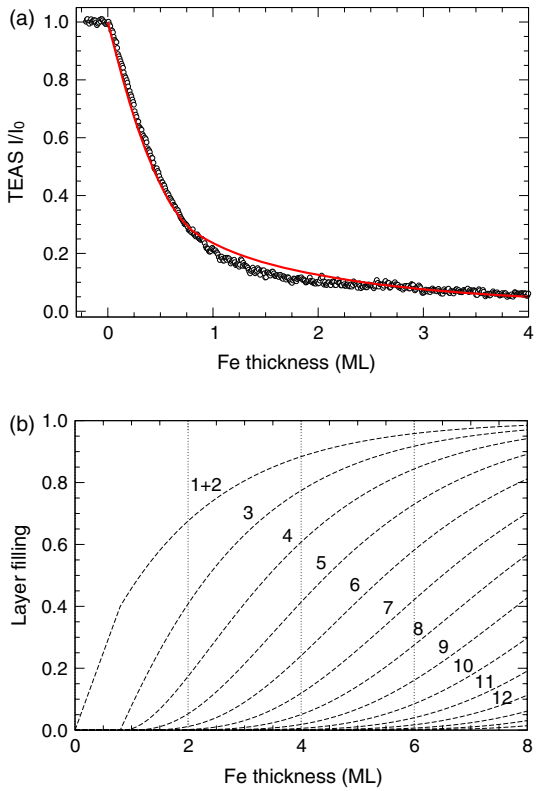


**Figure 1.** (a) Variation of the TEAS specular intensity during room temperature MBE growth of an Fe layer on Cu(111). The solid line is a fit to the data, using the structural model discussed in the text. (b) Evolution of atomic layer fillings during growth, as derived from our fit to the TEAS data.

front bears a striking resemblance to our own former results obtained on the growth of Co on Cu(111) [17].

The appearance of bilayer or even trilayer islands during the first stages of deposition has been observed not only for Fe [2, 3, 19] but also for Co on Cu [12, 20]. In this latter case, this phenomenon was shown to be caused by a strain-related destabilization of the epitaxial islands resulting in their breakup, accompanied by surface etching and alloy formation [13]. Beyond the third deposited layer, the Fe film is almost completely relaxed and has adopted its equilibrium bcc structure, as determined from LEED intensity versus energy ($I$–$V$) curves; our own measurements, not shown here, coincide with those previously reported [1, 19, 21]. It is important to remark that for Fe thicknesses well above 6 ML the Cu substrate is still not completely covered and bilayer formation continues, implying that substantial intermixing is still taking place at this stage. Atomic step crossings are hindered, as on many other compact metallic faces [22, 23] due to the existence of the so-called Ehrlich–Schwoebel energy barriers at the edges [14, 15]. As a consequence, the film grows in a very rough, multilayer fashion, forming pyramidal islands.

### *3.2. Surfactant-assisted growth of Fe on Cu(111)*

In our previous research on the growth of Co on Cu, we demonstrated the effectiveness of using a surfactant layer of Pb to improve the structural and morphological quality of

the Co films [17, 24, 25]. An attempt to apply the same method to the growth of Fe on Cu(111) found little structural improvement, at least during the early stages of growth [2, 3]. In this work we have extended the range of film thicknesses under study, in order to take full advantage of the ability of the TEAS technique to monitor the surface morphology in real time during deposition and the relative simplicity of our quantitative method of data analysis.

Using the same experimental procedure described above, we obtain the TEAS results presented in figure 2(a). Superimposed on an average trend of decreasing specular reflectivity which reveals a steady accumulation of disorder at the surface, similar to the case discussed above for the growth of Fe without surfactant, a maximum in the reflected intensity can now be seen for a deposited Fe thickness of 2 ML. Such a behavior indicates a reduced surface roughness at that point and a high filling of the exposed atomic levels, in a quasi-layer-by-layer fashion. This is confirmed by the results of our data analysis, presented in figure 2(b). Also in agreement with the previous work [2], these curves reveal that the interfacial FeCu bilayer is still formed in these films; therefore, the Pb surfactant does not completely prevent the breakup of the Fe islands as efficiently as it did with Co [26]. Nevertheless, we now find that the bilayer filling takes place much more rapidly, and the occupation of the third atomic layer starts later (for a total deposited thickness of ∼1.4 ML) than without the surfactant (∼0.9 ML). The subsequent growth of the Fe film in the presence of the Pb layer also proceeds with a smaller front width and hence a much reduced surface roughness. All these facts suggest an increased interlayer diffusion induced by the surfactant, as will be confirmed later on by our quantitative analysis of the data.

In an effort to understand the details of the surfactant effect on this system, a study using Monte Carlo (MC) simulations with many-body interatomic potentials [28] has been performed. This work will be published in full detail elsewhere [29]; here we only outline those results most relevant to interpret the experimental data. Contrary to the usual practice for the kinetic MC method, in which the different configurations are obtained by exchanging atomic positions within a fixed, discrete lattice, our simulations are carried out in continuum space; the atomic interactions are modeled using second-moment tight-binding (TB-SMA) interatomic potentials [30], which have been successfully used before to describe analogous systems [16]. In each iteration, the positions of all atoms in the simulated sample are shifted randomly by a small fraction of a lattice constant; the atomic displacements must therefore follow realistic trajectories in space. Newly generated configurations are accepted or rejected in the usual way, by computing their total energy and comparing the corresponding value of their Boltzmann factor with a random number. Again in agreement with our previous research of Co on Cu [13], no indications of single-atom interdiffusion of Fe at the flat areas of the Cu surface have been found in the simulations, either in the presence of a surfactant Pb layer or without it. Fe atoms can only be incorporated into the substrate from the upper side of a step, by pushing out an edge Cu atom. Thus, in the middle of

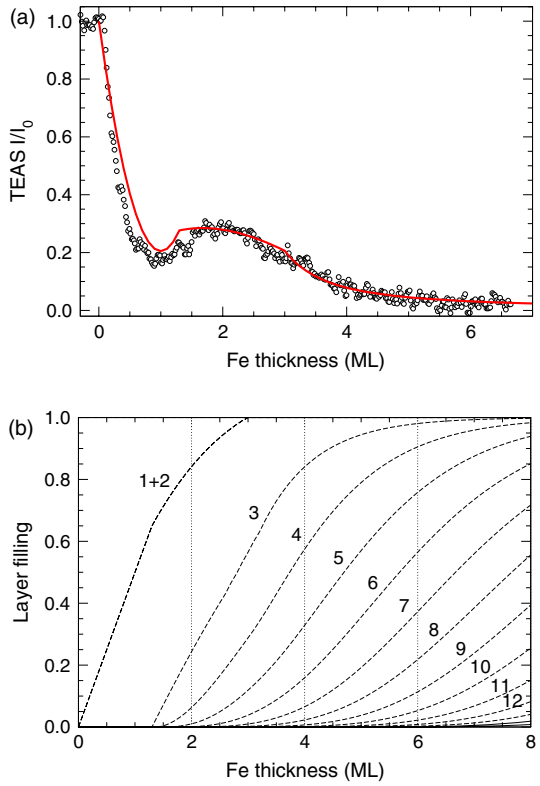


**Figure 2.** The same as in figure 1, but for an Fe layer grown on Cu(111) with the aid of a surfactant monolayer of Pb.

flat terraces the collective breakup of islands described above is the only mechanism leading to Fe–Cu intermixing. This phenomenon is demonstrated in figure 3. Here we show the final configuration of an initially flat, single-layer Fe island containing 24 atoms, and constructed underneath the surfactant Pb film. Immediately after starting the MC simulation, the Fe island becomes unstable and breaks up forming a double-layer cluster. Along with this process, which takes place below the surfactant, a Cu atom is pulled out of the substrate and incorporated into the island, resulting as expected in the formation of a mixed bilayer containing both Fe and Cu atoms.

The influence of kinetic parameters such as the deposition rate, which is very important for growth phenomena since they determine the density of nuclei, the average island size, etc [31], can hardly be captured with the MC technique due to the probabilistic nature of this latter. Still, the simulations are useful to reveal details about the film's crystallographic structure and its evolution with thickness. Figure 4 summarizes the results obtained for a 10 ML thick Fe film grown on a Cu(111) substrate covered by 1 ML Pb. In order to reproduce as closely as possible the experimental growth conditions, individual atoms were deposited one by one at random positions above the Pb layer and allowed to diffuse and accommodate for a number of MC steps before the arrival of the next adatom. They promptly penetrate below the Pb and perform some short diffusive displacements underneath it, which ensures that they are not frozen in an unstable configuration. To mimic the interdiffusion at the Fe–Cu interface, a mixed bilayer was first deposited with

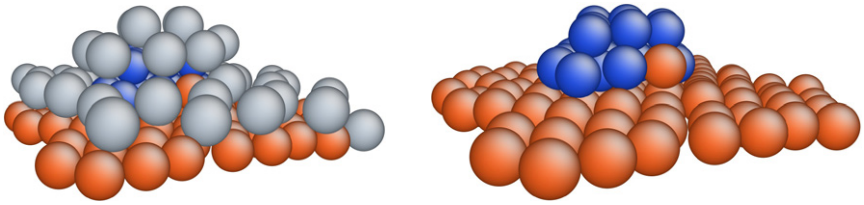

**Figure 3.** Result of a Monte Carlo simulation showing the formation of Fe islands of double atomic height through the destabilization of an initially single-layer island of 24 Fe atoms formed below the surfactant Pb film. The Cu atoms of the substrate are shown in pale gray (red online), Fe in dark gray (blue online); the larger spheres in the left-hand image are the surfactant Pb atoms[6] . A Pb atom can be seen filling in the vacancy left at the lower right corner by the Cu atom incorporated to the island. In the right-hand panel, the same island is shown after removing the Pb layer for clarity.

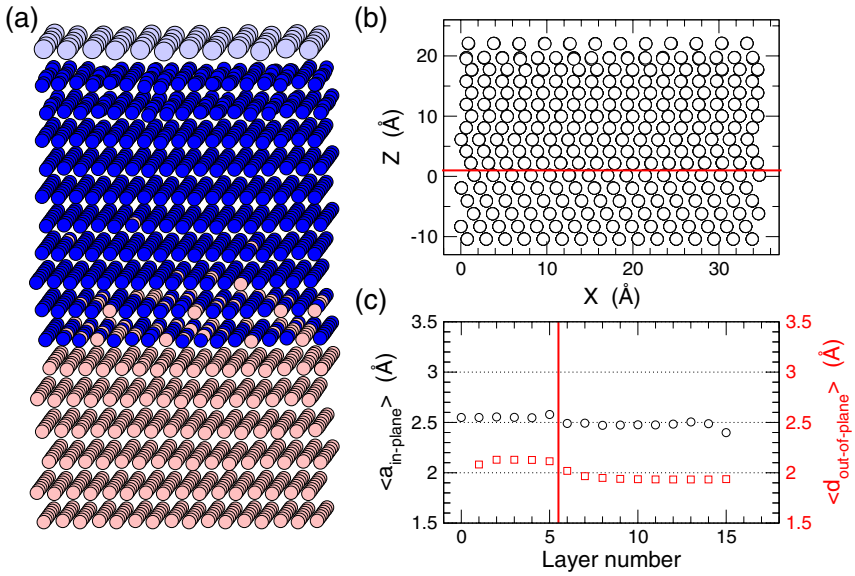


**Figure 4.** Results of Monte Carlo simulations of the growth of Fe on Cu(111) assisted by 1 ML of Pb as surfactant. (a) Pseudo-3D representation showing the atomic positions and their chemical identities. The atom types are denoted by the color code, bright (pink online) for Cu, dark (blue online) for Fe; the larger circles in the uppermost layer are Pb atoms. The interdiffused Fe–Cu interface is mimicked by a mixed bilayer with appropriate composition to ensure its stability, with pure Fe gradually deposited on top of it. (b) Lateral projection along the atomic rows demonstrating the stacking sequence; the inclusion of an additional atomic row of Fe accompanied by the formation of a dislocation at the Cu–Fe interface, and the appearance of stacking faults within the film are clearly visible. (c) Evolution of the in-plane nearest-neighbor (circles) and interplanar distances (squares) for the different atomic layers. The straight lines in (b) and (c) mark the position of the surface.

a composition (71% Fe, 29% Cu) that had previously been tested and shown to be structurally stable [29]; pure Fe was then added on top of this transition double layer. Figure 4(a) displays the actual atomic positions; Fe atoms are represented by blue circles, whereas Cu is displayed in pink. The appearance of dislocations at the interface to accommodate additional atomic rows can be directly visualized. The higher atomic density in the grown film helps release the strain due to the smaller lattice parameter of Fe as compared to that of Cu.

An analysis of the stacking sequence within the film (see the side view presented in figure 4(b)) shows that it maintains the fcc structure dictated by the Cu substrate, although with a high density of stacking faults which anticipates the transition from the fcc-(111) to the bcc-(110) following the Kurdjumov–Sachs (KS) epitaxial relation [1, 32]. This arrangement presents six domains, namely those orientations for which the $[\bar{1}1\bar{1}]_{bcc}$ direction is parallel to the $\{[\bar{1}01], [1\bar{1}0], [01\bar{1}]\}_{fcc}$, and those with the $[\bar{1}11]_{bcc}$ axis parallel to the $\{[0\bar{1}1], [10\bar{1}], [\bar{1}10]\}_{fcc}$ [32, 33]. Figure 4(c) finally shows the evolution of both the in-plane nearest-neighbor and interlayer spacings. While the perpendicular separation between Fe planes becomes stable at $1.93 \pm 0.01$ Å beyond the third deposited layer, the height of the first Fe plane sitting directly atop the Cu surface is substantially higher, namely $2.02 \pm 0.01$ Å. This might be an important piece of information for the interpretation of the magnetic data, since the atomic volume determines both the magnetic phase and the value of the magnetic moment per atom [6], and lattice deformations have a strong influence on magnetic anisotropies. Unfortunately we have not been able to confirm this result experimentally by means of either TEAS or LEED, due to the complexity of the measurements caused by the bilayer formation and the film roughness; more detailed measurements will be needed to settle this issue.

[6] Graphics produced with free AtomEye software, see [27].

More information can be derived from our measurements that deserves comment. In the Fe films grown with Pb interlayer diffusion is enhanced, albeit modestly, with respect to those deposited on clean Cu. The fit to the experimental TEAS data, depicted with a solid line in figure 2(a), yields a 48% probability for step crossings at RT. As demonstrated in previous work [13, 28] this effect basically results from a reduction of in-plane diffusion, rather than by facilitating step crossings. When trying to move below the Pb layer the diffusing adatoms find all neighboring sites blocked by the surfactant and consequently the probabilities of any displacements, either over a flat terrace or across a step become more similar than on the clean surface. At the same time, this reduced mobility of the deposited adatoms also leads to a higher density of nucleated islands that are smaller in size than without the surfactant; the total-step-length-to-thickness ratio is increased, which also facilitates step crossings. The enhanced diffusivity across the steps provoked by the surfactant explains the faster filling of atomic levels during growth and, in particular, the appearance of the maximum in the He beam reflectivity at 2 ML thickness, since the growing film is flattest at that point.

## 4. Magnetism

### *4.1. MOKE on Fe films grown on clean Cu(111)*

Once the structural and morphological characterization of the Fe films grown without and with surfactant have been completed, we move on to our study of their magnetic properties. It is well known from previous reports [19, 34] that during the first stages of growth of Fe on Cu(111) an fcc phase is formed with out-of-plane magnetization and a reduced atomic magnetic moment. Shortly after 2.0 ML thickness the Fe film starts to transform to bcc with in-plane magnetization and bulk-like magnetic moment. Our own MOKE data basically confirm those results, but the correlation of structural and magnetic measurements provides deeper insight into the transition process. We were not able to measure polar Kerr loops because our experiments were performed at 295 K, well above the Curie temperature of the perpendicularly magnetized Fe layers [35]. The black dots in figure 5 thus display the longitudinal Kerr intensity at saturation of the Fe films as a function of their thickness. We observe that the first in-plane magnetized patches of bcc Fe start to show up in the magnetic signal at ∼2.5 ML coverage. The Kerr intensity then rises steeply with increasing thickness as the fcc-to-bcc transformation proceeds and more regions of the Fe film progressively add their contribution to the total magnetic signal. An analogous behavior has been reported recently [36]. The minor differences in the thicknesses at which these features appear might be related to the sample preparation conditions. The slope break at ∼5 ML indicates the completion of the magnetic transformation; from this point on the MOKE signal continues to grow with a smaller slope that must correspond to the magnetic moment of bulk bcc Fe. This assumption is supported by the linearity of the data in the high thickness range and by their extrapolation to zero intensity (shown with a dashed line in the graph), which intercepts the horizontal axis at approximately 0.5 ML, suggesting that a significant fraction of the Fe at the interface is heavily mixed with Cu and remains non-magnetic.

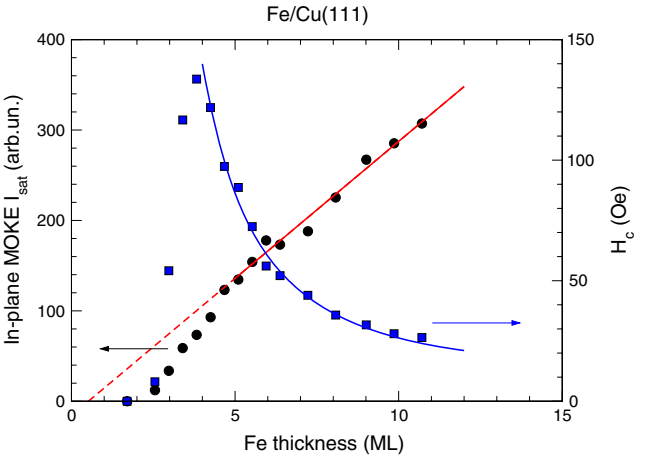


**Figure 5.** Saturation intensity (dots) and coercive field (squares) determined from longitudinal MOKE measurements at RT on Fe films grown on Cu(111). The solid lines are fits to the high thickness range in both sets of data, using a linear and a $t^{-2}$ model, respectively (see the text for details).

The evolution of the films' coercive field $H_c$ with Fe thickness is also depicted with squares in figure 5 and sensitively mirrors the structural and morphological changes taking place during growth. The first values measured right after the onset of the in-plane magnetic signal at 2.5 ML are very low, indicating that the Fe aggregates are quite small at this stage, barely surpassing their superparamagnetic limit, and disconnected from each other. We also know from the growth experiments described in section 3 that they are in fact mixed with Cu, which makes them magnetically softer and further reduces their coercivity [37]. Figure 1(b) demonstrates that at this thickness the Cu substrate is not yet completely covered, with the mixed FeCu bilayer occupying only 75% of the surface and the third level about 50%. As the bilayer fills in and the third layer islands grow in size and coalesce, $H_c$ increases following the evolution of the film's Curie temperature towards its bulk value [38]. After reaching a maximum of ∼135 Oe at about 4 ML, $H_c$ decreases as the last patches of the fcc structure disappear. This behavior has been theoretically modeled [39] showing that the increased coercivity in the transition region is due to the pinning of domain walls propagating through an inhomogeneous material containing regions of a different crystallographic structure. Even if the whole film seems to be bcc at 5 ML thickness, as deduced from the magnetization data, there must remain boundaries between islands or areas transformed at different stages; these defects gradually heal and disappear as growth continues, a process that is completed at about 11 ML. Our data for $H_c$ in this range approximately follow a $t^{-2}$ dependence with the Fe film thickness, as described by Chappert and Bruno [40], who also assigned it to the blocking of domain walls at structural defects. These magnetic data therefore constitute a sensitive probe revealing the progressive annihilation of defects as the film completes its structural transformation.

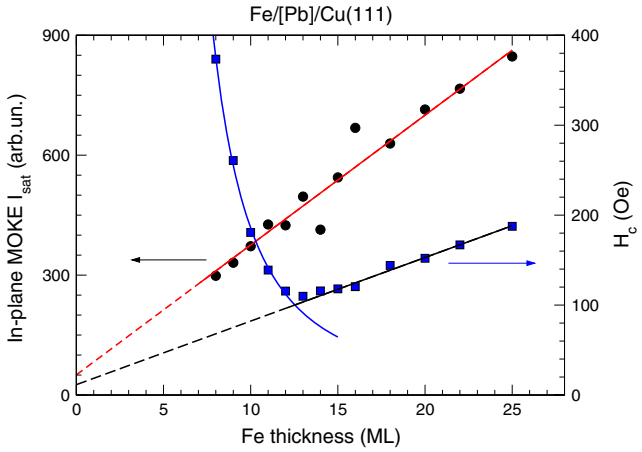


**Figure 6.** Saturation intensity and coercive field determined from longitudinal MOKE measurements at RT on Fe films grown on Cu(111) with the aid of a surfactant layer of Pb. The lines are fits to the data. Two regimes can be found for $H_c$: between ∼8 and ∼13 ML, $H_c$ decreases proportionally to $t^{-2}$, above 13 ML it grows linearly with $t_{Fe}$.

### *4.2. MOKE on Fe films grown on Cu(111) assisted by Pb*

Although the morphologies of the Fe films prepared with and without surfactant are not drastically different, which explains the apparent failure of the Pb surfactant to improve the quality of growth reported in the earlier study [2, 3], it must be kept in mind that even subtle structural changes can substantially affect the system's magnetic properties. Such a sensitive dependence can in turn be taken advantage of to tailor the material's properties by manipulating its structure. The coercivity of the Fe films grown with the aid of Pb is depicted by squares in figure 6, and reaches values much higher than in the Fe layers deposited directly on the Cu substrate. In fact, no data points could be obtained below 8 ML thickness because the magnetic field available in our system was not sufficient to saturate the samples. This higher coercivity must be caused by the smaller island size resulting from the reduced diffusivity provoked by the surfactant [28], which also increases the density of grain or island boundaries in spite of the reduced film roughness. The decrease of $H_c$ measured between ∼8 and ∼13 ML can also be approximated by a $t^{-2}$ law, but the healing process seems to be delayed by about 2 ML with respect to the Fe films grown without surfactant. At ∼13 ML coverage a different regime sets in and the coercivity starts to increase linearly with Fe thickness. This behavior should not be interpreted in terms of accumulation of defects in the film, since the fcc–bcc transition is already completed and our morphological characterization presented in figure 2 demonstrates that at this stage the growth front roughness is practically stabilized. The linear increase of the coercivity must therefore be mirroring the increase of the average grain size. While for large grains magnetization reversal is basically controlled by the magneto-crystalline anisotropy, in assemblies of very small grains the direct exchange interaction dominates and creates a reduced effective anisotropy by averaging over different grains [41]. In turn, the saturation MOKE intensity displayed with dots in figure 6 behaves linearly in the whole accessible data range. Its extrapolation towards zero thickness intercepts the vertical axis at a non-zero value, suggesting an enhancement of the magnetic moments at the interface; this observation will be discussed in the next section. In any case, it is clear that the interdiffusion of Fe into the Cu substrate, with its corresponding effect on the magnetic properties of the thinnest Fe films, has been substantially reduced by the presence of the surfactant.

## 5. Discussion

Several significant differences are apparent from a comparison between the magnetic data presented in figures 5 and 6. The first feature deserving attention is the absence of MOKE data at low thicknesses in the films grown with Pb. As discussed above in section 4.2, the presence of the surfactant reduces the mobility of the Fe adatoms, resulting in a higher density of islands with a smaller average size. Therefore, during the initial stages of growth the film must consist of an assembly of superparamagnetic clusters with blocking temperatures well below room temperature. Then, when percolation occurs the system suddenly evolves to a more or less continuous ferromagnetic film with a Curie temperature above 300 K but with a high concentration of defects (mostly island borders and unfilled voids), which contribute to domain wall pinning and thus enhance the film's coercivity.

Fe films grown without surfactant, in turn, form pyramidal islands with many partially filled atomic levels; hence, they relax more easily from the top and the appearance of the bcc structure takes place at a smaller deposited thickness. On the contrary, in the presence of Pb the bilayer at the interface grows and becomes completed more rapidly; the width of the growth front is also reduced by the enhanced interlayer diffusion, as demonstrated by figure 2. In this way the influence of the fcc substrate is maintained up to a higher Fe thickness, and the fcc–bcc transition is effectively retarded: a larger amount of Fe is required to reach the thickness necessary to unleash the transformation. The combination of these effects explains both the higher values of the coercivity measured on the Fe films grown with surfactant and the extension of the healing process. The fall of the coercivity takes about 2 ML longer in the Fe layers grown with Pb.

With respect to the $t^{-2}$ dependence of $H_c$, it should be mentioned that both sets of data (those of figures 5 and 6) are also compatible with the $t^{-4/3}$ law predicted by Néel [42]. This model, however, assumes a constant thickness fluctuation $dt/dx$ across the film (which we know is true for the Fe layers grown with surfactant, but not for those prepared on clean Cu), and Bloch magnetic domain walls, while in the thickness range of our experiments we expect these latter to be of Néel type [43].

The smaller size of the islands formed during surfactant-assisted growth can also explain the reduced interdiffusion observed in that case, on the basis of the collective mechanism illustrated in figure 3. Smaller islands accumulate less strain energy, and therefore pull out fewer Cu atoms from the substrate when they finally break up to form bilayer clusters. This Fe-richer mixed interface does indeed become magnetic

with increasing Fe thickness, and thus contributes to the total MOKE signal detected in our experiments, unlike the more heavily interdiffused layers formed when the Fe is grown without surfactant. The amount of magnetic Fe 'lost' due to interdiffusion in the samples grown without surfactant can be finely estimated to be around 0.5 ML from the extrapolation of our Kerr intensity data; this phenomenon should have a strong impact on the magnetic properties of multilayers.

It is interesting to remark that the deposition of the Fe at 65 K has been reported to lead to the formation of a low-spin, probably metastable distorted fcc layer [36]. At such a low temperature, atomic diffusion is nearly quenched, as demonstrated by the fractal shape of the islands observed, which also prevents intermixing by the collective mechanism described above. These results must therefore correspond to a layer of pure Fe directly in contact with the underlying Cu(111) surface, although no information is given in that work about the lattice parameters within the Fe film. On the contrary, our MOKE data displayed in figure 6 for the Fe/Cu(111) interface formed below the surfactant layer point towards an 'excess' magnetization that, albeit small, it is tempting to assign to an enhanced magnetic moment of the Fe atoms at the interface, resulting from the increased atomic volume reported in section 3.2, and/or to the appearance of some induced magnetic moments at the interfacial Cu atoms. Similarly increased magnetic moments have been reported in highly perfect Fe films grown on Cu(111) by ultrafast pulsed laser deposition (PLD) at 220 K [4]. If our hypothesis were correct, then our surfactant-assisted growth method would be capable of achieving analogous effects but with the Fe being deposited at room temperature and using the typical slow rates of MBE. X-ray magnetic circular dichroism (XMCD) experiments are under way to try to measure in detail the magnetic moments of all the atoms forming the interface and solve this issue.

## 6. Conclusions

We have demonstrated that by using a surfactant such as Pb during the growth of epitaxial Fe films on Cu some kinetic processes taking place during growth can be manipulated, thus enabling us to force the growth of metastable structures. Since even minor morphological and/or structural changes can substantially alter the magnetic behavior of the system, this technique can be used to help tailor the magnetic properties of low-dimensional materials such as multilayers or nanostructures. In particular, the coercivity of the Fe films grown on Cu(111) with the help of the surfactant could be raised by almost an order of magnitude, while their fcc-to-bcc transformation is delayed at least 2 ML. Furthermore, the amount of interdiffusion at the Fe–Cu interface is significantly reduced by the use of Pb, a feature that might be extremely useful for the preparation of high-quality, ultrathin magnetic heterostructures. Finally, an increased magnetic response is observed at the interface that could correspond to a high-spin phase of Fe.

## Acknowledgments

This work has been carried out within the framework of a collaborative program financed by the CEAL (Center for Latin American Studies). The participation of the Spanish group has also been partially supported by the MEC through grants FIS2007-61114, and NANOMAGNET S-0505/MAT/0194. The authors also gratefully acknowledge the Centro de Computación Científica de la Facultad de Ciencias (CCCFC) of the UAM for providing computing time through the *Moldyf* project.

## References

[1] Kief M T and Egelhoff W F Jr 1993 *Phys. Rev.* B **47** 10785
[2] Passeggi M C G Jr, Prieto J E, Miranda R and Gallego J M 2000 *Surf. Sci.* **462** 45
[3] Passeggi M C G Jr, Prieto J E, Miranda R and Gallego J M 2001 *Phys. Rev.* B **65** 035409
[4] Shen J, Ohresser P, Mohan Ch V, Klaua M, Barthel J and Kirschner J 1998 *Phys. Rev. Lett.* **80** 1980
[5] Moruzzi V L, Markus P M and Kubler J 1989 *Phys. Rev.* B **39** 6957
[6] García-Suárez V M, Newman C M, Lambert C J, Pruneda J M and Ferrer J 2004 *J. Phys.: Condens. Matter* **16** 5453
[7] Gradmann U, Kummerle W and Tillmanns P 1976 *Thin Solid Films* **34** 249
[8] Gradmann U and Tillmanns P 1977 *Phys. Status Solidi* a **44** 539
[9] Kummerle W and Gradmann U 1977 *Solid State Commun.* **24** 33
[10] Brodde A, Dreps K, Binder J, Lunau Ch and Neddermeyer H 1993 *Phys. Rev.* B **47** 6609
[11] Brodde A and Neddermeyer H 1992 *Ultramicroscopy* **42–44** 556
[12] de la Figuera J, Prieto J E, Ocal C and Miranda R 1994 *Surf. Sci.* **307–309** 538
[13] Gómez L, Slutzky C, Ferrón J, de la Figuera J, Camarero J, Vázquez de Parga A V, de Miguel J J and Miranda R 2000 *Phys. Rev. Lett.* **84** 4397
[14] Schwoebel R J and Shipsey E J 1966 *J. Appl. Phys.* **37** 3682
[15] Ehrlich G and Hudda F G 1966 *J. Chem. Phys.* **44** 1039
[16] Camarero J, Ferrón J, Cros V, Gómez L, Vázquez de Parga A L, Gallego J M, Prieto J E, de Miguel J J and Miranda R 1998 *Phys. Rev. Lett.* **81** 850
[17] de Miguel J J, Camarero J and Miranda R 2002 *J. Phys.: Condens. Matter* **14** 6155
[18] Camarero J, Cros V, Capitán M J, Álvarez J, Ferrer S, Niño M Á, Prieto J E, Gómez L, Ferrón J, Vázquez de Parga A L, Gallego J M, de Miguel J J and Miranda R 1999 *Appl. Phys.* A **69** 553
[19] Shen J, Klaua M, Ohresser P, Jenniches H, Barthel J, Mohan Ch V and Kirschner J 1997 *Phys. Rev.* B **56** 11134
[20] de la Figuera J, Prieto J E, Ocal C and Miranda R 1993 *Phys. Rev.* B **47** 13043
[21] Butterfield M T and Crapper M D 2003 *Surf. Sci.* **522** 167
[22] Giesen M 2001 *Prog. Surf. Sci.* **68** 1
[23] See, for instance, Ikonomov J, Starbova K and Giesen M 2007 *Surf. Sci.* **601** 1403 and references therein
[24] Camarero J, Spendeler L, Schmidt G, Heinz K, de Miguel J J and Miranda R 1994 *Phys. Rev. Lett.* **73** 2448
[25] de Miguel J J, Camarero J, de la Figuera J, Prieto J E and Miranda R 1998 *Morphological Organization in Epitaxial Growth and Removal* (*Series on Directions in Condensed Matter Physics* vol 14) ed Z Zhang and M G Lagally (Singapore: World Scientific) p 367

[26] Gómez L and Ferrón J 2001 *Phys. Rev.* B **64** 033409
[27] Li J 2003 *Modelling Simul. Mater. Sci.* **11** 173
[28] Ferrón J, Gómez L, Gallego J M, Camarero J, Prieto J E, Cros V, Vázquez de Parga A L, de Miguel J J and Miranda R 2000 *Surf. Sci.* **459** 135
[29] Gómez L, Ferrón J, de Miguel J J and Miranda R 2008 in preparation
[30] Tomanek D, Mukherjee S and Bennemann K H 1983 *Phys. Rev.* B **28** 665
[31] de Miguel J J, Ferrón J, Cebollada A, Gallego J M and Ferrer S 1988 *J. Cryst. Growth* **91** 481
[32] Kato M, Fukase S, Sato A and Mori T 1986 *Acta Metall.* **34** 1179
[33] Tian D, Jona F and Marcus P M 1992 *Phys. Rev.* B **45** 11216
[34] Kümmerle W and Gradmann U 1978 *Phys. Status Solidi* a **45** 171
[35] Huang F, Kief M T, Mankey G J and Willis R F 1994 *Phys. Rev.* B **49** 3962
[36] Torija M A, Gai Z, Myoung N, Plummer E W and Shen J 2005 *Phys. Rev. Lett.* **95** 027201
[37] Prieto J E, Camarero J, de Miguel J J, Miranda R, Rath Ch, Müller S, Hammer L and Heinz K 2000 *Appl. Phys. Lett.* **77** 889
[38] Camarero J, de Miguel J J, Miranda R and Hernando A 2000 *J. Phys.: Condens. Matter* **12** 7713
[39] Berger A, Feldmann B, Zillgen H and Wuttig M 1998 *J. Magn. Magn. Mater.* **183** 35
[40] Chappert C and Bruno P 1988 *J. Appl. Phys.* **64** 5736
[41] Herzer G 1990 *IEEE Trans. Magn.* **26** 1397
[42] Néel L 1956 *J. Phys. Rad.* **17** 250
[43] Methfessel S, Middelhoek S and Thomas H 1960 *IBM J. Res. Dev.* **4** 96